VIA MEDICA

ORIGINAL PAPER

Folia Histochem Cytobiol
Vol. 62, No. 3, 2024, pp. 123–132

DOI: 10.5603/fhc.101592
ISSN 0239-8508, e-ISSN 1897-5631

Changes in early endosomes in rat hippocampal CA1 neurons after transient global cerebral ischaemia

Min Qiang[1,*], Bai-Hong Tan[2,*], De-Sheng Huo[1], Shu-Lei Li[1], Zi-Zhen Fan[1], Ze-Qun Zhou[1], Rong-Yu Wang[1], Yan-Chao Li[1]

[1]Department of Histology and Embryology, College of Basic Medical Sciences, Norman Bethune Health Science Centre of Jilin University, Changchun City, Jilin Province, PR China

[2]Laboratory Teaching Centre of Basic Medicine, Norman Bethune Health Science Centre of Jilin University, Changchun City, Jilin Province, PR China

*These authors contributed equally to this work.

ABSTRACT

Introduction. Transient global ischaemia in rodents causes selective loss of hippocampal CA1 neurons, but the potential involvement of endocytic pathways has not been fully explored. The aim of this study was to investigate the changes in early endosomes in the CA1 subfield after ischaemia and reperfusion.

Material and methods. A four-vessel occlusion (4-VO) model was established in Wistar rats to induce 13 minutes of global cerebral ischaemia. Neuronal death was detected by Fluoro-Jade B (FJ-B) staining at various intervals after reperfusion, and intracellular membrane changes in ischaemic neurons were revealed using $DiOC_6(3)$, a lipophilic fluorescent probe. Ras-related protein Rab5 (Rab5) immunostaining was performed to detect changes in early endosomes in ischaemic neurons. Western blot analysis was used to confirm the morphological observations on Rab5 in the CA1 hippocampal subfield.

Results. FJ-B staining confirmed progressive neuronal death in the CA1 subfield in ischaemic rats after reperfusion. $DiOC_6(3)$ staining revealed abnormally increased membranous components in ischaemic CA1 neurons. Specifically, early endosomes, as labelled by Rab5 immunostaining, significantly increased in number and size in CA1 neurons at 1.5 and 2 days post-reperfusion, followed by rupture at day 3 and a decrease in staining intensity at day 7 post-reperfusion. Western blot analysis confirmed a significant upregulation of Rab5 protein levels at day 2, which returned to near control levels by day 7.

Conclusions. Our study revealed significant changes in the dynamics of early endosomes in CA1 neurons after ischaemia-reperfusion injury. The initial increase in the area fraction of early endosomes in CA1 neurons may reflect an upregulation of endocytic activity, whereas the fragmentation and reduction of early endosomes at the later stage may indicate a failure of adaptive mechanisms of ischaemic neurons against ischaemia-induced death. Understanding the temporal dynamics of early endosomes provides critical insights into the cellular mechanisms that govern fate of CA1 hippocampal neuronsl after ischaemia/reperfusion.

Keywords: rat; transient global cerebral ischaemia; CA1; damaged neurons; endosomes; Rab5

Correspondence address:
Yan-Chao Li
Department of Histology and Embryology, College of Basic Medical Sciences,
Norman Bethune Health Science Centre of Jilin University,
126 Xinmin Street, Changchun City, Jilin Province 130021, PR China
e-mail: liyanchao@jlu.edu.cn

Submitted:
15 July, 2024
Accepted after reviews:
12 September, 2024
Available as Online first:
25 September, 2024

INTRODUCTION

A temporary disruption in cerebral blood flow can result in delayed death of vulnerable neurons, especially in the hippocampus [1–3]. In animals experiencing global cerebral ischaemia, autophagosomes and lysosomes were observed to increase in number and size in ischaemic neurons, indicating enhanced cellular degradation following ischaemia [4, 5]. However, the effects of ischaemia on endocytic pathways are less studied. Investigating these impacts could illuminate mechanisms of neuronal damage and suggest new therapeutic approaches [6].

The endosomal pathway within neurons is a tightly controlled and efficient system for the uptake and processing of extracellular nutrients, growth factors, and receptors [7–9]. It also plays a role in the recovery and degradation of plasma membrane integrins following neurotransmitter releases, ensuring that relevant information is relayed to intracellular biosynthetic pathways [10]. Moreover, endocytosis in neurons serves to internalise components of the plasma membrane that have been damaged, which is a vital process for maintaining the functionality of the neural membrane [11]. This complex system underscores the sophisticated mechanisms that neurons employ to manage their internal and external environment, facilitating their survival and proper functioning.

Endosomes are classified into early and late stages based on the timing of endocytosis and the expression of certain markers [12]. Ras-associated binding (Rabs) proteins, a family of small GTP-binding proteins, play a critical role in regulating the structure and function of the endosomal system by recruiting specific effector proteins to different vesicular surfaces [13–15]. Rab5, predominantly located on early endosomes, serves as a key marker for early endosomes [16, 17]. Therefore, examining changes in Rab5 distribution and content within neurons can reveal the extent of external stress on neurons and provide valuable insights into the mechanisms underlying neuronal damage.

Previous studies on Alzheimer's disease have shown a strong link between dysfunction of endocytosis and neuronal death [18, 19]. However, the changes in endocytosis and its relationship with ischaemia-induced neuronal death remain largely unclear. Understanding this connection will offer new insights and perspectives on the mechanisms underlying ischaemia-induced neuronal death.

Materials and methods

Ethical approval

The experiment was approved by the Animal Research Committee of Jilin University, China, (Permit Number: SYXK (Ji) 2022-0015) and was performed according to the National Institute of Health Guide for the Care and Use of Laboratory Animals [20].

Four-vessel occlusion (4-VO) cerebral ischaemia/reperfusion (I/R) model

This model was operated on the principle of inducing global cerebral ischaemia in rats by electrocoagulating the vertebral arteries through the pterygoid foramen of the first cervical vertebra under ether anaesthesia. Additionally, reversible clips were loosely applied to both common carotid arteries [21]. After 24 hours, the rat, now conscious, was restrained, and the clips on the carotid arteries were tightened to achieve occlusion of all 4 vessels. Blood flow was restored after removing the carotid artery clamps for periods of 13 min [22, 23].

The efficacy of the 4-vessel occlusion (4-VO) whole-brain ischaemia model varied depending on rat strains and their feeding conditions, because these factors can influence the extent of delayed neuronal death. Variations can occur even within the same strain under different feeding conditions, leading to inconsistent experimental outcomes [24, 25]. To mitigate these variables, we chose the Wistar rat, the most commonly utilised strain in this experimental model, for its established reliability and consistency in experimental ischaemia studies. Previous studies and our own findings have shown that in the 4-VO cerebral ischaemia model, occlusion of the bilateral common carotid arteries for 15 min or longer raised the risk of rat tics and mortality [26–29]. Therefore, we selected a 13-minute closure time to reduce these risks while still effectively studying ischaemic effects [22]. This model offered several advantages, including straightforward animal preparation, a high rate of ischaemic neuronal damage, a low incidence of seizures, and the absence of anaesthesia effects on the experimental outcomes [30].

Animal groups

A total of 62 Wistar rats (2 months old, male, 250–270 g) were used in this experiment. Among them, 50 rats were subjected to the ischaemic operation, and 12 rats were used as sham-operated controls. Of the 50 ischaemic rats, 37 rats survived from the 13-min-long global cerebral ischaemia. The rats were randomly divided into 8 groups, each consisting of 6 rats. Five groups were designated for morphological analysis: the sham control group, and experimental groups for 1.5, 2, 3, and 7 days post-ischaemia. The remaining 3 groups were set aside for protein analysis, including the sham group and experimental groups for days 2 and 7 post-ischaemia. This approach allowed for a comprehensive analysis of both morphological changes and protein expression alterations at various time points following ischaemia, providing insights into the dynamics of neuronal injury and recovery.

Animal and tissue processing for morphological analysis

Experimental animals were anaesthetised with 10% chloral hydrate administered intraperitoneally (*i.p.*, 400 mg/kg).

The thoracic cavity was opened to reveal the heart, and a perfusion pump was used to flush the circulatory system with physiological saline through the ascending aorta. The right atrial appendage was cut open so that blood and saline could flow out. This was followed by perfusion fixation for about 10 min using 4% paraformaldehyde. After the perfusion process, the brain was extracted and submerged in 4% paraformaldehyde for 4–6 h for post-fixation at 4°C, and then washed in a series of cold sucrose solutions of increasing concentration until they sunk to the bottom of the vessel. Brain tissues were transversely sectioned into slices of 30–50 μm thickness using a cryostat (Tissue-Tek, Sakura Finetek, Tokyo, Japan). The brain sections from Bregma –2.28 to –4.68 mm, which contained the dorsal hippocampus, were selected and rinsed 3 times with 0.1 M phosphate buffer (PB, pH 7.4), with each rinse lasting 5–15 min, and subsequently stored at 4°C.

Detection of I/R-induced neuronal cell death with Fluoro-Jade B staining (FJ-B)

To examine neuronal death, a series of sections were processed for FJ-B staining (Immu-Mount, Thermo Fisher Scientific, Rockford, IL, USA), and observed under an Olympus BX53 F microscope equipped with a digital imaging system (Olympus, Tokyo, Japan), as described previously [31]. FJ-B is a widely used fluorochrome that selectively stains degenerating neurons in brain slices. The histochemical application of FJ-B is simple, sensitive, and reliable, making it suitable for detecting neuronal degeneration [32]. As compared to conventional methods, such as haematoxylin-eosin (H&E) or Nissl staining, this technique is more sensitive and specific in detecting neuronal degeneration caused by neurotoxic insults.

$DiOC_6(3)$ staining plus immunostaining for the early endocytic marker Rab5

$DiOC_6(3)$ (D273) was purchased from Thermo Fisher (Shanghai, China). Sections were pretreated with 10% normal donkey serum in 0.1 M PB containing 0.1% Triton X-100 at room temperature for 30 min. Subsequently, they were incubated with rabbit polyclonal anti-Rab5 monoclonal IgG (1:500, early endosomal marker ab18211; Abcam, Waltham, MA, USA) overnight at 4°C. The next day, the sections were washed 3 times with 0.1 M PB, and then labelled with Alexa Fluor™ 594 donkey anti-rabbit antibody (1:500, Molecular Probes, Eugene, OR, USA) and 2.5 μg/mL $DiOC_6(3)$ in 0.1 M PB at room temperature, protected from light, for 1 h.

Phalloidin staining plus immunostaining for the early endocytic marker Rab5

A series of sections were arranged in a 24-well plate and washed 3 times with 0.1 M PB for 10 min each. The sections were incubated in 300 μL of a mixture containing 10% donkey serum and 0.3% Triton X-100 in 0.1 M PB in each well for 1 h at room temperature to block nonspecific sites. Without washing, the sections were then incubated with a rabbit anti-Rab5 at 1:500 dilution overnight at 4°C After several washes, the sections were incubated with Alexa 594-conjugated donkey anti-rabbit secondary antibody (1:500, Molecular Probes) and Alexa 488-conjugated phalloidin (1:100, A12379, Molecular Probes) for 2 h at room temperature in the dark. After washing with 0.1M PB, the sections were mounted with IMMU-MOUNT (Immu-Mount, USA).

Morphological analysis of the changes in Rab5 in hippocampal CA1 neurons

Stained sections were observed using an Olympus FV1000 confocal laser scanning microscope (Olympus, Tokyo, Japan). High-power confocal micrographs, taken with a 60× objective at 2× optical zoom, were used for detailed analysis. Quantitative analysis was performed on the raw images, which were not adjusted for brightness or contrast. The images were imported into Image-Pro Plus 6.0 software to measure the area fraction occupied by Rab5--positive structures in each neuron in the CA1 subfield, as described previously [33, 34]. Briefly, the area positive for Rab5 and the corresponding cytoplasmic area were measured in at least 20 CA1 pyramidal cells for each section. At least 4 sections were scored for each animal and 6 rats were analysed in each group. The ratio of the area occupied by Rab5-positive particles to the cytoplasmic area was measured for each neuron and calculated from the combined data of all animals in each group.

Western blot analysis of the early endosomal marker, Rab5

To assess the change of Rab5 at the protein level, 4 sham-operated and 8 ischaemic rats were deeply anaesthetised with chloral hydrate (*i.p.* 400 mg/kg) on days 2 and 7 after ischaemia (n = 4 *per* group). The brains were removed and cut in a cold buffer into 300 μm-thick transverse slices containing the dorsal hippocampus between –1.30 and –4.80 mm from Bregma. The CA1 subfield was microdissected from the CA3 + dentate gyrus (DG) portion under a Leica MZ6 stereomicroscope (Leica Systems Inc., Buffalo Grove, IL, USA) and kept separately at –80°C until use.

Equal amounts of protein samples were separated on 12% SDSPAGE, and then transferred to polyvinylidene fluoride membranes (PVDF, Pall, BSP0161, USA). The membranes were blocked with 5% bovine serum albumin in Tris-buffered saline containing 0.1% Tween-20 for 2 h, and then incubated with rabbit polyclonal anti-Rab5 monoclonal IgG (1:1000, ab18211; Abcam) overnight at 4°C. As a reference protein, glyceraldehyde-3-phosphate dehydrogenase (GAPDH) was probed with mouse monoclonal anti-GAPDH IgM (1:1000, Boster Biological Technology, Wuhan, Hubei, China).

The membranes were further labelled with peroxidase-conjugated affiniPure F(ab')$_2$ fragment of goat anti-rabbit IgG (H+L) (Jackson ImmunoResearch Laboratories, West Grove, PA, USA), visualized by ECL detection kit (34080, SuperSignal™, Thermo Fisher, USA) and analysed using Quantity One software (version 4.6.2).

Statistical analysis

All data were expressed as mean ± SEM across the groups and statistically analysed using SPSS version 18.0 packadge (Chicago, IL, USA). Differences between the ischaemic and control groups were statistically assessed using One-Way analysis of variance (ANOVA), followed by Tukey's multiple comparison test with a significance threshold of $P < 0.05$, enabling a precise evaluation of the impact of ischaemia on neurons.

RESULTS

Ischaemia-induced neuronal death in the CA1 subfield of the hippocampus

In this study, we assessed the damage to hippocampal neurons by staining with FJ-B, a fluorescent marker known for its specific binding to dying or dead neurons. As shown in Figure 1, no FJ-B-positive cells were observed in the hippocampus of sham-operated controls (Fig. 1A1–A2). However, at 1.5 days post-reperfusion, a subset of cells in the pyramidal layer of the CA1 subfield in ischaemic rats showed modest FJ-B positivity (Fig. 1B1). At this stage, FJ-B fluorescence was localised to the perikaryal cytoplasm, and the cells retained their typical morphology (Fig. 1B2). By day 2 post-reperfusion, most cells in the CA1 subfield were intensely FJ-B stained (Fig. 1C1), and these neurons showed significant morphological damage, including atrophy and distortion (Fig. 1C2). FJ-B-positive neurons were consistently detected in the CA1 subfield at days 3 to 7 post-reperfusion (Fig. 1E1-E2). At day 7, ischaemia-induced damage progressed to the CA3 subfield of the hippocampus, while the intensity of FJ-B staining in CA1 neurons was significantly reduced at this time point (Fig. 1E2).

Ischaemia-induced changes in membranous components in CA1 neurons

FJ-B is not readily adaptable to double fluorescence analysis because of the need to pre-treat sections with ethanol and potassium permanganate solutions. As an alternative, a membrane-bound dye, $DiOC_6(3)$, which has been reported to be able to detect neuronal death [35], was used in this study to reveal ischaemia-damaged neurons.

Examination of $DiOC_6(3)$-stained sections revealed that some CA1 cells became positively stained at 1.5 days post-reperfusion. $DiOC_6(3)$-positive structures were distributed in the perikaryal cytoplasm of CA1 cells, whose nuclei remained negative. $DiOC_6(3)$-positive cells were consistently observed up to day 7 (Fig. 2D1, E1), the longest time point examined in this study, but the intensity of staining in CA1 neurons was somewhat reduced at day 7 after reperfusion (Fig. 2E1).

Unlike FJ-B staining, $DiOC_6(3)$ staining has a unique mechanism whereby it specifically binds to the hydrophobic domain in the phospholipid bilayer of biomembranes [35]. Therefore, the increase in $DiOC_6(3)$ staining indicated abnormalities in intracellular membranes in CA1 neurons induced by ischaemia and reperfusion. Consistently, $DiOC_6(3)$ staining plus immunostaining for Rab5 showed that early endosomes were significantly increased in number and size in the $DiOC_6(3)$-positive cells in the CA1 subfield at 1.5 days after reperfusion (Fig. 2B2). The increase in Rab5 immunostaining persisted until day 3 but was reduced in intensity by day 7 after reperfusion (Fig. 2D2, E2).

Morphological and protein analysis of early endosome changes in hippocampal CA1 neurons

To further investigate the changes in early endosomes of hippocampal CA1 neurons, we performed an analysis using immunostaining for Rab5 plus phalloidin staining on hippocampal sections (Fig. 3). Phalloidin, a fluorescent probe, specifically binds to filamentous actin (F-actin), which is predominantly located beneath the neuronal cell membrane. Because hippocampal CA1 neurons exhibit atrophy and deformation following ischaemia/reperfusion, phalloidin staining was used to clearly define cell boundaries.

Figure 3F2–J2 shows a series of high-power confocal micrographs illustrating changes in early endosomes within CA1 neurons over a 7-day period following ischaemia/reperfusion. Neuronal contours were revealed by phalloidin staining (Fig. 3F1–J1). In the sham-operated control group, only a few Rab5-positive particles were observed, scattered throughout the perikaryal cytoplasm of CA1 neurons (Fig. 3A2, F2). Compared with the sham group, there was a marked increase in the number of Rab5-positive particles in CA1 neurons of ischaemic rats at 1.5 days post-reperfusion (Fig. 3B2, G2). A significant increase in both the number and size of Rab5-positive particles was observed in ischaemic CA1 neurons at day 2, with neurons filled with numerous large particles (Fig. 3C2, H2). However, the punctate staining pattern of Rab5 immunostaining in CA1 neurons disappeared by day 3 after reperfusion, and the cytoplasm of CA1 neurons showed diffuse staining (Fig. 3D2, I2). A similar diffuse staining pattern was observed in CA1 neurons at day 7 post-reperfusion, but the staining intensity was significantly reduced (Fig. 3E2, J2). It is noteworthy that from day 2 to day 7 after reperfusion, the cell bodies of the CA1 neurons showed a significant degree of distortion and atrophy (Fig. 3C1–E1, H1–J1), as compared to those in the sham-operated controls (Fig. 3A1, F1). Quantitative analysis showed that the area fraction of Rab5-positive structures significantly increased

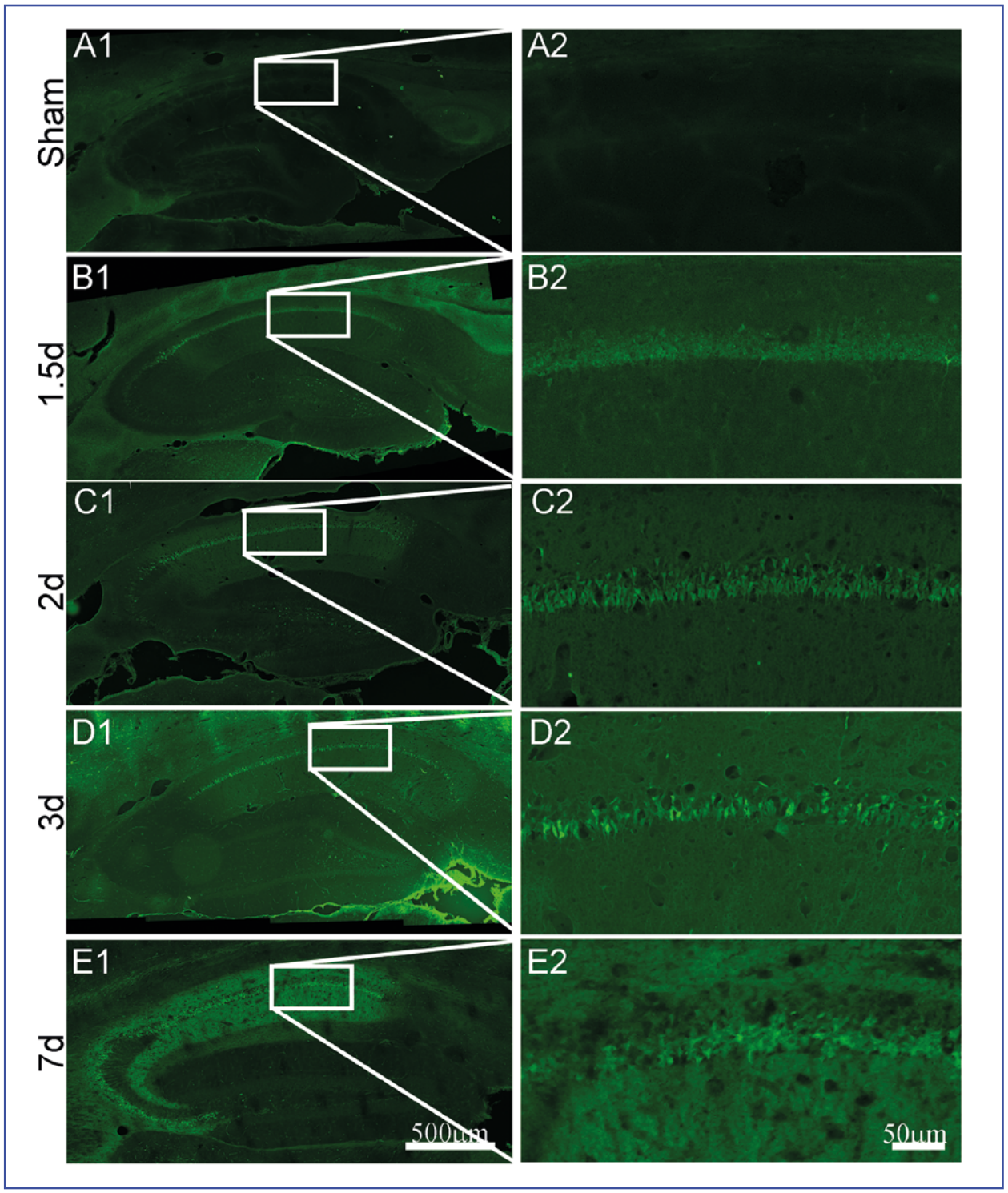

Figure 1. FJ-B staining in the rat hippocampus following transient global cerebral ischaemia. FJ-B is used to detect dying or dead neurons in the hippocampus of both sham and experimental groups at 1.5, 2, 3, and 7 days after reperfusion. **A1–E1.** FJ-B staining throughout the hippocampus, and the CA1 subfield in A1–E1 (partially boxed) is further magnified in **A2–E2**, showing the progression of CA1 neuronal death. Scale bars: A1–E1: 500 μm; A2–E2: 50 μm.

at 1.5 day ($P < 0.05$), peaked at 3 days ($P < 0.001$), and remained higher at 7 days post-reperfusion ($P < 0.01$, $n = 6$), compared to the sham-operated control group (Fig. 4A).

Western blot analysis (Fig. 4B) was performed on both sham and experimental groups to quantify Rab5 protein and confirm the results of anti-Rab5 immunostaining. The results showed that the protein level of Rab5 was significantly elevated in the ischaemic group on day 2 ($P < 0.01$), but returned to near the level of the sham control group by day 7 after reperfusion ($P > 0.05$, $n = 4$).

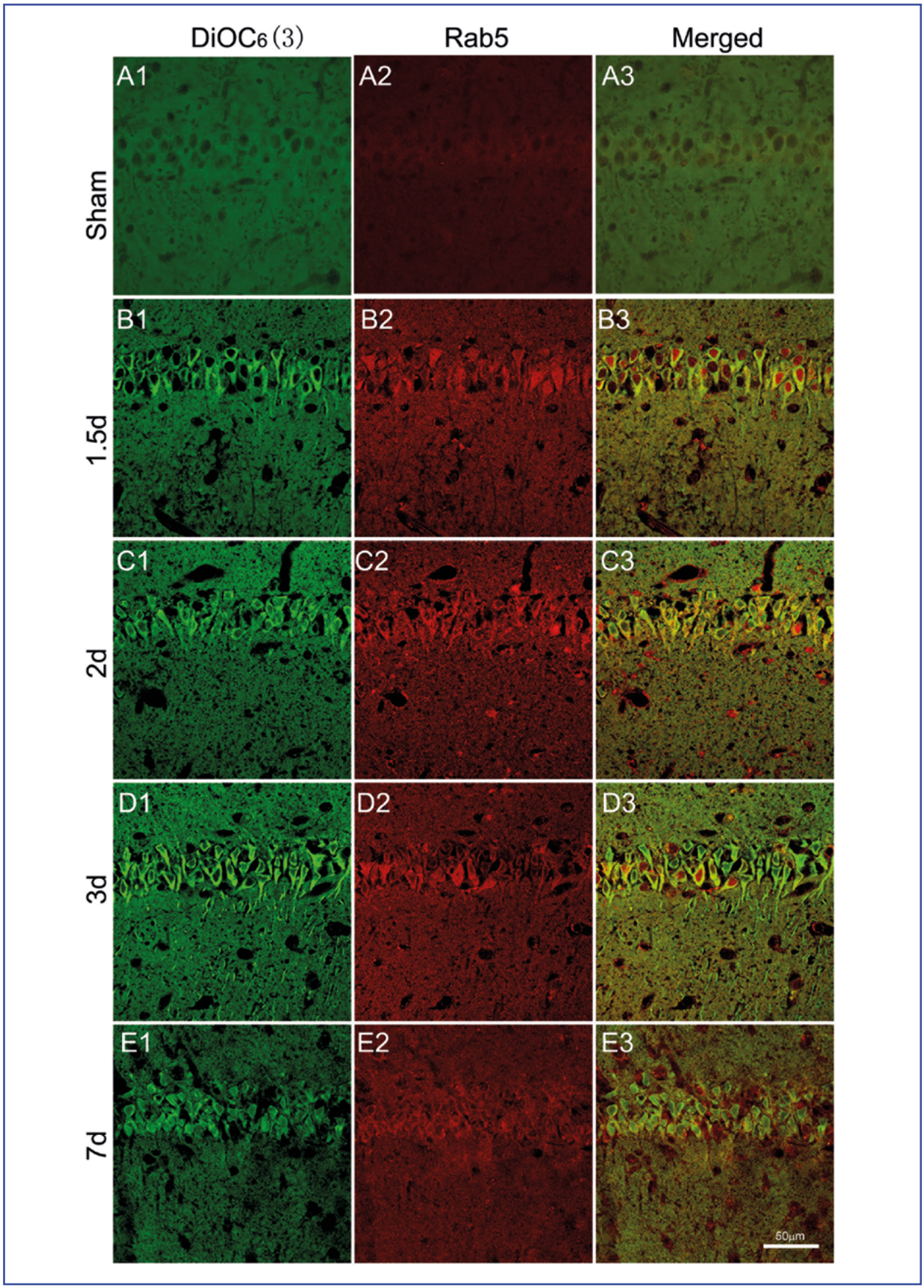

Figure 2. $DiOC_6(3)$ staining combined with immunostaining for Rab5 in the CA1 subfield of the rat hippocampus following transient global cerebral ischaemia. **A1–E1.** $DiOC_6(3)$ staining in the sham and ischaemic rats from 1.5 to 7 days after reperfusion. **A2–E2.** Immunostaining for Rab5 in the sham and ischaemic rats from 1.5 to 7 days after reperfusion. **A3–E3.** Are merged from A1–E1 and A2–E2, respectively. Scale bars: 50 μm.

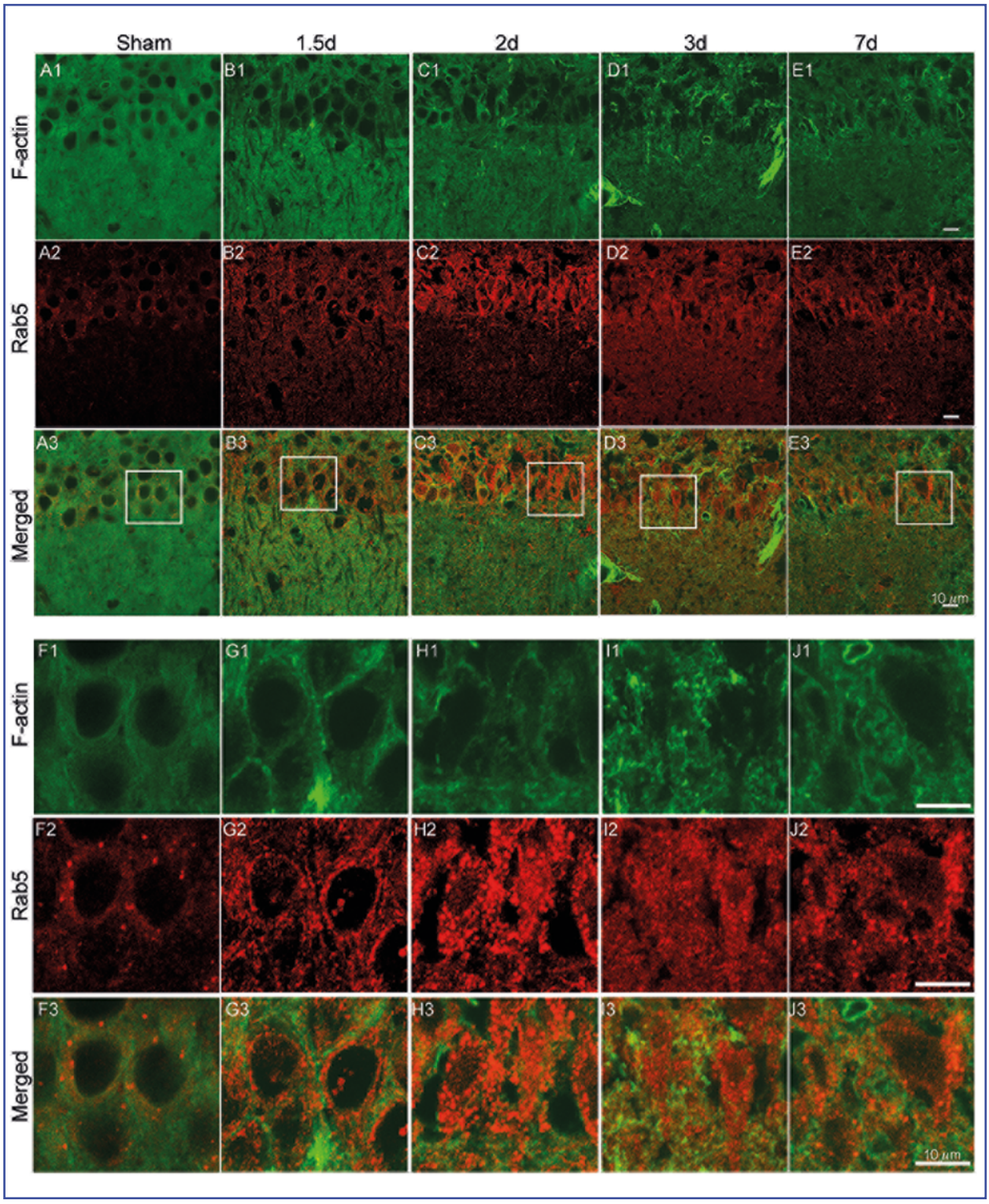

Figure 3. Confocal images showing the changes in the distribution of F-actin and Rab5 in CA1 neurons after ischaemia/reperfusion. **A1–E1.** Phalloidin staining in CA1 neurons in the sham and ischaemic rats at 1.5 to 7 days after I/R. **A2–E2.** Immunostaining for Rab5 in the sham and ischaemic rats at 1.5 to 7 days after I/R. **A3–E3** are merged form **A1–E1** and **A2–E2**, respectively. **F1–J1**, **F2–J2**, **F3–J3** are the enlarged images of **A1–E1**, **A2–E2**, **A3–E3** at the selected position of the box, repectively. Scale bars: 10 μm.

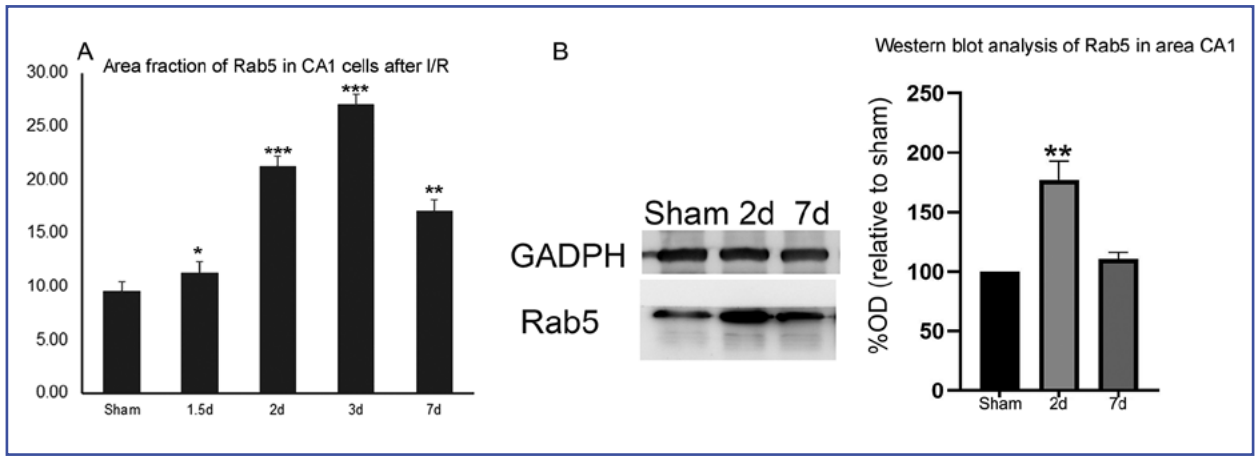

Figure 4. Morphological and protein analysis of Rab5 in the CA1 subfield of the hippocampus. **A.** The area fractions of Rab5-positive structures in CA1 neurons are compared between sham and ischaemic rats from 1.5 to 7 days after reperfusion. $^{*}P < 0.5$; $^{**}P < 0.01$; $^{***}P < 0.001$, relative to the sham-operated control (n = 6 *per* group, one-way ANOVA). **B.** Western blot analysis was conducted on Rab5 in the CA1 subfield of the hippocampus in both sham-operated and ischaemic rats at days 2 and 7 after reperfusion. $^{**}P < 0.001$, relative to the sham-operated control (n = 4 *per* group, one-way ANOVA). Abbreviation: GAPDH — glyceraldehyde-3-phosphate dehydrogenase.

Discussion

Transient global cerebral ischaemia in rodents is a well-established model that specifically induces neuronal loss in the hippocampal CA1 subfield, with cell death typically occurring between 48 and 72 hours after ischaemia and reperfusion [1–3, 36, 37]. Our findings, as revealed by FJ-B staining, are consistent with the existing literature and confirm the delayed progression of hippocampal neuronal death in this study [36]. $DiOC_6(3)$, a lipophilic dye that binds to the hydrophobic regions of phospholipids in biomembranes, was previously reported to reveal an increase in membrane components within dying or dead neurons in the ischaemic hippocampal CA1 subfield [38]. Our $DiOC_6(3)$ staining similarly indicates an increase in membranous elements, suggesting that perturbations in cellular membrane integrity occurred as early as 1.5 days after ischaemia/reperfusion.

Cerebral ischaemia, characterised by reduced blood flow to the brain, is known to trigger a cascade of events including energy failure, ion pump dysfunction, and excitotoxicity, particularly in vulnerable brain regions, ultimately leading to neuronal death [37]. Neurons in the central nervous system (CNS), with their extensive synaptic connections, rely heavily on the transport of materials to the soma for degradation, placing high demands on the endolysosomal degradation pathway [6]. Endocytosis is a cellular process central to the internalisation of nutrients, neurotransmitters, and membrane proteins, as well as the regulation of cell surface receptors [35]. The complexity of the endosomal system makes it vulnerable to dysfunction, which has been demonstrated as a hallmark of various neurodegenerative diseases, especially those affecting the CNS [39–41].

Rab5, a member of the Ras superfamily of small GTPases, is critical for early endosome fusion and proper functioning of the endocytic pathway [13–15]. Using Rab5 as a molecular marker for early endosomes, we observed a significant increase in the number and size of early endosomes in hippocampal CA1 neurons of ischaemic animals between 1.5 and 2 days after reperfusion. Increased immunostaining for Rab5 overlapped with $DiOC_6(3)$ staining in CA1 neurons, suggesting that increased endocytosis may contribute to the observed increase in membranous structures in ischaemic neurons.

As a key regulator of early endocytic events, Rab5 serves as both a marker of early endosomes and an indicator of the cell's ability to manage endocytic cargo [16, 17], therefore reflecting cellular homeostasis and the potential for neuronal dysfunction. Although some CA1 neurons were positive for FJ-B or $DiOC_6(3)$ staining as early as 1.5 days after reperfusion, cell atrophy and distortion were evident until the second day after reperfusion [36]. Given this, the initial increase in the area fraction of Rab5-positive particles in CA1 neurons may reflect an upregulation of endocytic activity at the early stage of reperfusion, as described in Alzheimer's disease [18, 19]. This may be a response by ischaemic neurons to maintain cellular homeostasis and counteract ischaemia-induced cell death. In support of this, our Western blotting analysis confirms that Rab5 protein levels were significantly elevated in the CA1 subfield of ischaemic rats on day 2 after reperfusion.

As reperfusion continued, the Rab5 staining pattern in ischaemic CA1 neurons became diffuse and blurred. This phenomenon is indicative of endosomal rupture and may be attributed to autolysis caused by lysosomal leakage, which is common in ischaemic neurons at this stage [42]. The rupture of early endosomes suggests a failure of the adaptive mechanisms of ischaemic neurons against ischaemia-induced death at the stage or reperfusion. Despite a significant decrease in the size of Rab5-positive particles,

the area fraction of Rab5 immunopositivity remained elevated at days 3 and 7 after reperfusion due to diffuse cytoplasmic staining. However, our Western blot analysis confirmed that Rab5 protein levels had returned to near normal levels in the CA1 subfield of ischaemic rats by day 7 post-reperfusion.

Our study has revealed significant changes in the dynamics of early endosomes in CA1 neurons following ischaemia-reperfusion injury. To our knowledge, the detailed changes in early endosomes following ischaemia have not been previously reported. The initial increase in the area fraction of early endosome is thought to be part of the neuron's reparative mechanisms to restore cellular homeostasis, while the fragmentation and reduction of early endosomes at days 3–7 after reperfusion may be associated with compromised integrity of the endolysosomal system. Because it occurs in a spatiotemporal manner consistent with overt neuronal death, dysfunction of the endolysosomal system is likely to be a critical event marking the transition from reversible to irreversible neuronal injury. Understanding the temporal dynamics of early endosomes provides critical insights into the cellular mechanisms that govern neuronal fate following ischaemic events, which may provide a clue for the development of targeted therapeutic strategies aimed at preserving endolysosomal function and promoting neuronal survival in conditions of cerebral ischaemia.

Article information and declarations

Data availability statement

The data that support the findings of this study will be made available on request from the corresponding author.

Ethics statement

The experiment was approved by the Animal Research Committee of Jilin University (Permit Number: SYXK (Ji) 2022-0015) and was performed according to the National Institute of Health Guide for the Care and Use of Laboratory Animals.

Author contributions

All authors contributed to the study conception and design. Material preparation, data collection, and analysis were performed by BHT, DSH, SLL, ZZF, ZQZ, RYW, and YCL. The first draft of the manuscript was written by MQ. MQ, BHT, ZZF, RYW prepared Figures 1–4. All authors commented on previous versions of the manuscript. All authors read and approved the final manuscript. YCL agreed to be accountable for all aspects of the work in ensuring that questions related to the accuracy or integrity of any part of the work are appropriately investigated and resolved.

Funding

This work was supported by Natural Science Foundation, Department of Science and Technology of Jilin Province of China (Grant Number: 20240101268JC, to YC Li).

Conflict of interest

The authors declare that the research was conducted in the absence of any commercial or financial relationships that could be construed as a potential conflict of interest.

REFERENCES

1. Hartman RE, Lee JM, Zipfel GJ, et al. Characterizing learning deficits and hippocampal neuron loss following transient global cerebral ischemia in rats. Brain Res. 2005; 1043(1-2): 48–56, doi: 10.1016/j.brainres.2005.02.030, indexed in Pubmed: 15862517.
2. Ito U, Spatz M, Walker JT, et al. Experimental cerebral ischemia in mongolian gerbils. I. Light microscopic observations. Acta Neuropathol. 1975; 32(3): 209–223, doi: 10.1007/BF00696570, indexed in Pubmed: 1180003.
3. Endres M, Engelhardt B, Koistinaho J, et al. Improving outcome after stroke: overcoming the translational roadblock. Cerebrovasc Dis. 2008; 25(3): 268–278, doi: 10.1159/000118039, indexed in Pubmed: 18292653.
4. Adhami F, Schloemer A, Kuan CY. The roles of autophagy in cerebral ischemia. Autophagy. 2007; 3(1): 42–44, doi: 10.4161/auto.3412, indexed in Pubmed: 17035724.
5. Chen W, Sun Y, Liu K, et al. Autophagy: a double-edged sword for neuronal survival after cerebral ischemia. Neural Regen Res. 2014; 9(12): 1210–1216, doi: 10.4103/1673-5374.135329, indexed in Pubmed: 25206784.
6. Hu K, Gaire BP, Subedi L, et al. Interruption of endolysosomal trafficking after focal brain ischemia. Front Mol Neurosci. 2021; 14: 719100, doi: 10.3389/fnmol.2021.719100, indexed in Pubmed: 34650402.
7. O'Sullivan MJ, Lindsay AJ. The endosomal recycling pathway — at the crossroads of the cell. Int J Mol Sci. 2020; 21(17), doi: 10.3390/ijms21176074, indexed in Pubmed: 32842549.
8. Huotari J, Helenius A. Endosome maturation. EMBO J. 2011; 30(17): 3481–3500, doi: 10.1038/emboj.2011.286, indexed in Pubmed: 21878991.
9. Scott CC, Vacca F, Gruenberg J. Endosome maturation, transport and functions. Semin Cell Dev Biol. 2014; 31: 2–10, doi: 10.1016/j.semcdb.2014.03.034, indexed in Pubmed: 24709024.
10. Schreij AMA, Fon EA, McPherson PS. Endocytic membrane trafficking and neurodegenerative disease. Cell Mol Life Sci. 2016; 73(8): 1529–1545, doi: 10.1007/s00018-015-2105-x, indexed in Pubmed: 26721251.
11. Eichel K, Uenaka T, Belapurkar V, et al. Endocytosis in the axon initial segment maintains neuronal polarity. Nature. 2022; 609(7925): 128–135, doi: 10.1038/s41586-022-05074-5, indexed in Pubmed: 35978188.
12. Bonifacino JS, Rojas R. Retrograde transport from endosomes to the trans-Golgi network. Nat Rev Mol Cell Biol. 2006; 7(8): 568–579, doi: 10.1038/nrm1985, indexed in Pubmed: 16936697.
13. Small SA, Schobel SA, Buxton RB, et al. A pathophysiological framework of hippocampal dysfunction in ageing and disease. Nat Rev Neurosci. 2011; 12(10): 585–601, doi: 10.1038/nrn3085, indexed in Pubmed: 21897434.
14. Tang BL. Rabs, membrane dynamics, and Parkinson's disease. J Cell Physiol. 2017; 232(7): 1626–1633, doi: 10.1002/jcp.25713, indexed in Pubmed: 27925204.
15. Barz S, Kriegenburg F, Sánchez-Martín P, et al. Small but mighty: Atg8s and Rabs in membrane dynamics during autophagy. Biochim Biophys Acta Mol Cell Res. 2021; 1868(9): 119064, doi: 10.1016/j.bbamcr.2021.119064, indexed in Pubmed: 34048862.
16. Xu W, Fang F, Ding J, et al. Dysregulation of Rab5-mediated endocytic pathways in Alzheimer's disease. Traffic. 2018; 19(4): 253–262, doi: 10.1111/tra.12547, indexed in Pubmed: 29314494.
17. Langemeyer L, Fröhlich F, Ungermann C. Rab GTPase function in endosome and lysosome biogenesis. Trends Cell Biol. 2018; 28(11): 957–970, doi: 10.1016/j.tcb.2018.06.007, indexed in Pubmed: 30025982.
18. Huang Y, Lemke G. Early death in a mouse model of Alzheimer's disease exacerbated by microglial loss of TAM receptor signaling. Proc Natl Acad Sci U S A. 2022; 119(41): e2204306119, doi: 10.1073/pnas.2204306119, indexed in Pubmed: 36191221.
19. Colacurcio DJ, Pensalfini A, Jiang Y, et al. Dysfunction of autophagy and endosomal-lysosomal pathways: roles in pathogenesis of Down syndrome and Alzheimer's Disease. Free Radic Biol Med. 2018;

114: 40–51, doi: 10.1016/j.freeradbiomed.2017.10.001, indexed in Pubmed: 28988799.
20. National Research Council (US) Institute for Laboratory Animal Research. Guide for the care and use of laboratory animals. National Academies Press, Washington 1996.
21. Zhang Y, Tan BH, Wu S, et al. Different changes in pre- and postsynaptic components in the hippocampal CA1 subfield after transient global cerebral ischemia. Brain Struct Funct. 2022; 227(1): 345–360, doi: 10.1007/s00429-021-02404-7, indexed in Pubmed: 34626230.
22. Pulsinelli WA, Brierley JB. A new model of bilateral hemispheric ischemia in the unanesthetized rat. Stroke. 1979; 10(3): 267–272, doi: 10.1161/01.str.10.3.267, indexed in Pubmed: 37614.
23. Xu D, Bureau Y, McIntyre DC, et al. Attenuation of ischemia-induced cellular and behavioral deficits by X chromosome-linked inhibitor of apoptosis protein overexpression in the rat hippocampus. J Neurosci. 1999; 19(12): 5026–5033, doi: 10.1523/JNEUROSCI.19-12-05026.1999, indexed in Pubmed: 10366635.
24. Bernardeau M, Vernoux JP. Overview of differences between microbial feed additives and probiotics for food regarding regulation, growth promotion effects and health properties and consequences for extrapolation of farm animal results to humans. Clin Microbiol Infect. 2013; 19(4): 321–330, doi: 10.1111/1469-0691.12130, indexed in Pubmed: 23445377.
25. Petito CK, Pulsinelli WA, Jacobson G, et al. Edema and vascular permeability in cerebral ischemia: comparison between ischemic neuronal damage and infarction. J Neuropathol Exp Neurol. 1982; 41(4): 423–436, doi: 10.1097/00005072-198207000-00005, indexed in Pubmed: 7086465.
26. Anderova M, Vorisek I, Pivonkova H, et al. Cell death/proliferation and alterations in glial morphology contribute to changes in diffusivity in the rat hippocampus after hypoxia-ischemia. J Cereb Blood Flow Metab. 2011; 31(3): 894–907, doi: 10.1038/jcbfm.2010.168, indexed in Pubmed: 20877389.
27. de Oliveira JN, Reis LO, Ferreira ED, et al. Postischemic fish oil treatment confers task-dependent memory recovery. Physiol Behav. 2017; 177: 196–207, doi: 10.1016/j.physbeh.2017.05.009, indexed in Pubmed: 28483394.
28. Kovalenko T, Osadchenko I, Nikonenko A, et al. Ischemia-induced modifications in hippocampal CA1 stratum radiatum excitatory synapses. Hippocampus. 2006; 16(10): 814–825, doi: 10.1002/hipo.20211, indexed in Pubmed: 16892187.
29. Ancer-Rodríguez J, Villarreal-Silva EE, Salazar-Ybarra RA, et al. Four-vessel occlusion model using aged male Wistar rats: a reliable model to resolve the discrepancy related to age in cerebral ischemia research. Anat Sci Int. 2016; 91(3): 226–237, doi: 10.1007/s12565-015-0286-x, indexed in Pubmed: 25966656.
30. Elkin SR, Lakoduk AM, Schmid SL. Endocytic pathways and endosomal trafficking: a primer. Wien Med Wochenschr. 2016; 166(7-8): 196–204, doi: 10.1007/s10354-016-0432-7, indexed in Pubmed: 26861668.
31. Schmued LC, Albertson C, Slikker W. Fluoro-Jade: a novel fluorochrome for the sensitive and reliable histochemical localization of neuronal degeneration. Brain Res. 1997; 751(1): 37–46, doi: 10.1016/s0006-8993(96)01387-x, indexed in Pubmed: 9098566.
32. Schmued LC. Development and application of novel histochemical tracers for localizing brain connectivity and pathology. Brain Res. 2016; 1645: 31–35, doi: 10.1016/j.brainres.2016.03.053, indexed in Pubmed: 27155454.
33. Zhang YF, Xiong TQ, Tan BH, et al. Pilocarpine-induced epilepsy is associated with actin cytoskeleton reorganization in the mossy fiber-CA3 synapses. Epilepsy Res. 2014; 108(3): 379–389, doi: 10.1016/j.eplepsyres.2014.01.016, indexed in Pubmed: 24559838.
34. Xiong T, Liu J, Dai G, et al. The progressive changes of filamentous actin cytoskeleton in the hippocampal neurons after pilocarpine-induced status epilepticus. Epilepsy Res. 2015; 118: 55–67, doi: 10.1016/j.eplepsyres.2015.11.002, indexed in Pubmed: 26600371.
35. Deshpande LS, Lou JK, Mian A, et al. Time course and mechanism of hippocampal neuronal death in an in vitro model of status epilepticus: role of NMDA receptor activation and NMDA dependent calcium entry. Eur J Pharmacol. 2008; 583(1): 73–83, doi: 10.1016/j.ejphar.2008.01.025, indexed in Pubmed: 18289526.
36. Guo CY, Xiong TQ, Tan BH, et al. The temporal and spatial changes of actin cytoskeleton in the hippocampal CA1 neurons following transient global ischemia. Brain Res. 2019; 1720: 146297, doi: 10.1016/j.brainres.2019.06.016, indexed in Pubmed: 31233713.
37. Kirino T. Ischemic Tolerance. J Cereb Blood Flow Metab. 2002; 22(11): 1283–1296, doi: 10.1097/01.WCB.0000040942.89393.88, indexed in Pubmed: 12439285.
38. Wu S, Zhang YF, Gui Y, et al. A novel detection method for neuronal death indicates abnormalities in intracellular membranous components in neuronal cells that underwent delayed death. Prog Neurobiol. 2023; 226: 102461, doi: 10.1016/j.pneurobio.2023.102461, indexed in Pubmed: 37179048.
39. Ghavami S, Shojaei S, Yeganeh B, et al. Autophagy and apoptosis dysfunction in neurodegenerative disorders. Prog Neurobiol. 2014; 112: 24–49, doi: 10.1016/j.pneurobio.2013.10.004, indexed in Pubmed: 24211851.
40. Rivero-Ríos P, Romo-Lozano M, Fasiczka R, et al. LRRK2-related Parkinson's disease due to altered endolysosomal biology with variable Lewy body pathology: a hypothesis. Front Neurosci. 2020; 14: 556, doi: 10.3389/fnins.2020.00556, indexed in Pubmed: 32581693.
41. Jordan KL, Koss DJ, Outeiro TF, et al. Therapeutic targeting of rab GTPases: relevance for Alzheimer's disease. Biomedicines. 2022; 10(5), doi: 10.3390/biomedicines10051141, indexed in Pubmed: 35625878.
42. Neumann JT, Cohan CH, Dave KR, et al. Global cerebral ischemia: synaptic and cognitive dysfunction. Curr Drug Targets. 2013; 14(1): 20–35, doi: 10.2174/138945013804806514, indexed in Pubmed: 23170794.